SAND2015-0811C

Spurious effects of analog-to-digital conversion nonlinearities on radar range-Doppler maps

A. W. Doerry[*], D. F. Dubbert[†], B. L. Tise[‡]

Sandia National Laboratories, P.O. Box 5800, MS 0519, Albuquerque, NM 87185

ABSTRACT

High-performance radar operation, particularly Ground Moving Target Indicator (GMTI) radar modes, are very sensitive to anomalous effects of system nonlinearities. System nonlinearities generate harmonic spurs that at best degrade, and at worst generate false target detections. One significant source of nonlinear behavior is the Analog to Digital Converter (ADC). One measure of its undesired nonlinearity is its Integral Nonlinearity (INL) specification. We examine in this paper the relationship of INL to radar performance; in particular its manifestation in a range-Doppler map or image.

Keywords: radar, spurs, ADC, analog-to-digital, interference, nonlinearity

1 INTRODUCTION

Radar data and data products often exhibit extraordinarily large dynamic ranges. Synthetic Aperture Radar (SAR) images can be well beyond 100 dB. Even Ground Moving Target Indicator (GMTI) range-Doppler maps exhibit dynamic ranges routinely above 80 dB. With GMTI data, we are often looking for small targets that manifest barely above the noise level, but still in the presence of other large target energies.[1] This is especially true for Dismount-detection GMTI (DMTI). Achieving this level of dynamic range requires an extraordinarily linear radar channel.

One inescapably nonlinear component is the Analog to Digital Converter (ADC). The ADC's quantization function is indeed nonlinear, but can be readily accommodated if it exhibits known (generally uniform) quantization steps. However, if the quantization steps are unknown, that is other than that which is presumed, albeit usually bounded to some fraction of the nominal quantization step size, then we might expect anomalous effects in the radar data. This typically will manifest as undesirable harmonic spurs in the range-Doppler map, leading to increased false alarms and reduced detection probability for GMTI operation.

The unknown and undesired nonlinearity aspects of an ADC are embodied in the ADC's Differential Nonlinearity (DNL) and its Integral Nonlinearity (INL) specifications. Inadequate performance in this regard can be particularly problematic for GMTI operation, and is in fact not uncommon. GMTI modes are particularly sensitive because we are often trying to detect very weak targets against the noise floor of the radar. Other component specifications also address ADC nonlinearity.[2]

What follows is an analysis of INL effects, as manifests in a range-Doppler map, with the assumption of stretch processing having been employed.[3] We will further assume Intermediate Frequency (IF) sampling with digital down-conversion, a common technique for high-performance radar systems. This paper summarizes an earlier report on the topic.[4]

[*] awdoerr@sandia.gov; phone 505-845-8165; www.sandia.gov/radar

[†] dfdubbe@sandia.gov; phone 505-845-8424

[‡] bltise@sandia.gov; phone 505-284-9736

2 DISCUSSION – INTEGRAL NONLINEARITY

A good primer on Integral Nonlinearity (INL) is an Application Note by Maxim Integrated Products, Inc.[5]

2.1 What is it?

The ideal transfer function for an ADC is a stair-step function, where ADC output codes exhibit constant increments with uniform step sizes in input voltage. Quantization is said to be uniform. The centers of such steps are linear, that is, on a straight line. Alas, real ADCs exhibit steps that are not on a straight line. We desire components that minimize nonlinear behavior.

The nonuniformity of the individual steps is recorded as a Differential Nonlinearity (DNL). The accumulation of the nonlinear steps indicates the departure of the actual ADC transfer function from a straight line, and is recorded as the Integral Nonlinearity (INL). Both INL and DNL are typically reported as fractions of the Least-Significant Bit (LSB) of the ADC. They may also sometimes be reported as fractions or percent of Full Scale Range (FSR). It is particularly important to remember that that the LSB metric in absolute terms does in fact depend on the number of bits in the ADC. Nevertheless, INL and DNL are simply measures of the nonlinear behavior of the ADC, beyond merely sampling and quantizing the data in a uniform fashion. Measurement of INL and DNL is addressed in an Application Note from Analog Devices.[6]

2.2 How Does it Manifest in the Sampled Data?

This is all about relating an INL spec to ADC sample values in a mathematical sense.

2.2.1 Digital Down-Conversion – Ideal ADC

We begin with a single ADC operating at some sampling frequency which we identify as f_s. The sample period is the inverse of this, namely

$$T_s = 1/f_s \ = \text{ADC fast-time sample period.} \tag{1}$$

It is particularly convenient for the input signal to be at an IF center frequency of $f_s/4$. Consequently, we identify the real-valued IF signal as

$$x_{IF}(t) = x(t)e^{j2\pi(f_s/4)t} + x^*(t)e^{-j2\pi(f_s/4)t}, \tag{2}$$

where $x^*(t)$ is the complex conjugate of $x(t)$. Furthermore, $x(t)$ is typically band-limited to something less than $f_s/2$, and often to less than $f_s/4$. The ADC samples this signal at uniformly spaced sample times and generates data samples ideally described by

$$x_{ADC}(n) = x_{IF}(T_s n), \tag{3}$$

where n is the sample index value. Note that $x_{ADC}(n)$ is also real-valued. The digital down-conversion (demodulation) is typically implemented as the complex multiplication

$$x_{dem}(n) = e^{-j(\pi/2)n}\left[x_{ADC}(n)\right]. \tag{4}$$

Combining the previous results yields the signal of interest, namely

$$x_{dem}(n) = x(T_s n) + x^*(T_s n)e^{-j\pi n}. \tag{5}$$

This normally undergoes additional low-pass filtering to remove the $e^{-j\pi n}$ modulated term, and typically some data decimation as well. We model the demodulated and filtered signal as

$$x_{demfil}(n) = x_{dem}(n) * h_{demfil}(n) \approx x(T_s n) \ , \tag{6}$$

where $h_{demfil}(n)$ is the demodulator filter. It is this term $x_{demfil}(n) \approx x(n/f_s)$ that is of interest to us for further processing.

2.2.2 Digital Down-Conversion – ADC With INL

The development begins as in the previous section, but departs at the point of describing the ADC samples. The new description includes an error term due to INL. That is

$$x_{ADC}(n) = x_{IF}(T_s n) + \varepsilon_{INL}\left(x_{IF}(T_s n)\right), \tag{7}$$

where $\varepsilon_{INL}(z)$ is the error added to the ideal signal due to INL. We note that the error in $x_{ADC}(n)$ depends on the instantaneous value for $x_{ADC}(n)$ itself. Ideally, we desire $\varepsilon_{INL}(z) = 0$. Failing that, we desire the effects of $\varepsilon_{INL}(z)$ be negligible in the range-Doppler map, especially in GMTI modes. As before, the digital down-conversion is implemented as the complex multiplication. Combining the previous results yields the signal of interest, namely

$$x_{dem}(n) = \left[x(T_s n) + x^*(T_s n) e^{-j\pi n} + e^{-j(\pi/2)n} \varepsilon_{INL}\left(x_{IF}(T_s n)\right) \right]. \tag{8}$$

This normally undergoes additional low-pass filtering to remove the $e^{-j\pi n}$ modulated term, and typically some data decimation as well. We again model the filtered signal as in Eq. (6). Expanding the result yields

$$x_{demfil}(n) \approx x(T_s n) + \left[\left\{ e^{-j(\pi/2)n} \varepsilon_{INL}\left(x_{IF}(T_s n)\right) \right\} * h_{demfil}(n) \right]. \tag{9}$$

The term within the square brackets represents the impact of INL on the data. Some comments are in order

- The INL affects the data generally in an annoyingly nonlinear fashion. Therein lays the problem.
- The nonlinear function is the calculation of $\varepsilon_{INL}\left(x_{IF}(T_s n)\right)$. After that, all operations are linear again.
- The effects of INL of consequence are those that make it through the filter $h_{demfil}(n)$, after a frequency shift by $e^{-j(\pi/2)n}$. If the filter were perfect, then it is only the INL effects that make it through the passband. Otherwise, we also need to include perhaps effects that are significant even after stopband attenuation.

2.2.3 Details of Signal Conversion – Ideal ADC

In the foregoing analysis, we have assumed that the ideal conversion was the assignment of sample values based on Eq. (3). We now explore this in somewhat more detail. We shall assume that the ADC conversion range is limited to the region $-1/2 \le x_{IF}(T_s n) < 1/2$. However, the ADC conversion function operates on some range of voltages, and assigns output code values consistent with 0 for the most negative signal value, and $2^{b_{ADC}} - 1$ for the most positive signal value, where b_{ADC} = number of bits in the ADC. The ADC output is quantized to $2^{b_{ADC}}$ different values, hopefully with constant step sizes. We define the conversion operation with the function

$$Z = Q(z, b_{ADC}), \tag{10}$$

where z is the analog input with range $0 \le z < 1$, and Z is the assigned quantized output with range $0 \le Z < 1$. We also define the ideal uniform quantization step size then as

$$q = 2^{-b_{ADC}} . \tag{11}$$

The conversion operation in practice produces a quantization error. That is, for an ideal ADC, this error is

$$\varepsilon_q \left(z, b_{ADC} \right) = Z - z . \tag{12}$$

The transfer function is defined to be linear and without error when $\varepsilon_q \left(kq, b_{ADC} \right) = 0$, where k = integer, that is $k \in I$, and $0 \le k < 2^{b_{ADC}}$. Consequently, we can infer that for an ideal ADC,

$$Q\left(kq, b_{ADC} \right) - kq = 0 . \tag{13}$$

We note that in this case $-q/2 \le \varepsilon_q \left(z, b_{ADC} \right) < q/2$. For complex (in the 'complicated' sense) signals, this error is uniformly distributed, and uncorrelated (white). We like this, and strive to make this happen even for low-level signals with dither signals. Given all this, we can relate a more accurate ideal conversion operation as

$$x_{ADC}\left(n \right) = x_{IF}\left(T_s n \right) + \varepsilon_q \left(\left(x_{IF}\left(T_s n \right) + \frac{1}{2} \right), b_{ADC} \right) . \tag{14}$$

However, statistically, since the average quantization error is zero, we can generally presume $x_{ADC}\left(n \right) = x_{IF}\left(T_s n \right)$.

2.2.4 Details of Signal Conversion – ADC with INL

In the previous development for an ideal ADC, we stipulated that the quantization error $\varepsilon_q \left(kq, b_{ADC} \right) = 0$. We now depart from this assumption, and allow $\varepsilon_q \left(kq, b_{ADC} \right) \ne 0$. In particular, we identify the residual error as its own function

$$\varepsilon_q \left(kq, b_{ADC} \right) = g\left(kq \right) . \tag{15}$$

We identify the nature of $g\left(kq \right)$ to be a smoothed residual error, that is, interpolated between sample values of argument $\left(kq \right)$. Recall that the general quantization error will be a stair-step function for a continuum of ADC input values. An important distinction is that $\varepsilon_q \left(z, b_{ADC} \right)$ is a stair-step function (albeit with perhaps nonuniform steps), and $g\left(z \right)$ is an interpolated residual error. The equality of these two holds only at argument values $z = kq$. We define a new error as

$$\varepsilon_{q'} \left(z, b_{ADC} \right) = \varepsilon_q \left(z, b_{ADC} \right) - g\left(z \right) . \tag{16}$$

Of course, this new error behaves more like the quantization error from an ideal ADC. That is, it exhibits a stair-step behavior with $\varepsilon_{q'} \left(kq, b_{ADC} \right) = 0$. Nevertheless, the actual quantization error is now the sum of this idealized quantization error and the interpolated residual error, that is

$$\varepsilon_q \left(z, b_{ADC} \right) = \varepsilon_{q'} \left(z, b_{ADC} \right) + g\left(z \right) . \tag{17}$$

Given all this, we identify our new conversion operation as

$$x_{ADC}(n) = x_{IF}(T_s n) + \varepsilon_{q'}\left(\left(x_{IF}(T_s n) + \frac{1}{2}\right), b_{ADC}\right) + g\left(x_{IF}(T_s n) + \frac{1}{2}\right). \tag{18}$$

However, as before, the idealized quantization error is statistically zero, so we can generally presume

$$x_{ADC}(n) = x_{IF}(T_s n) + g\left(x_{IF}(T_s n) + \frac{1}{2}\right). \tag{19}$$

With respect to the earlier development, we identify the INL error as

$$\varepsilon_{INL}\left(x_{IF}(T_s n)\right) = g\left(x_{IF}(T_s n) + \frac{1}{2}\right). \tag{20}$$

More commonly, an INL specification will present a sample plot with abscissa units between zero and full-scale, and ordinate units of Least Significant Bit (LSB). We identify such a typical INL specification function, in units of LSB, as $G(w)$, where w is the abscissa, with $0 \le w < fs$, where fs is the full-scale value of ADC input (not to be confused with sampling frequency). We relate the typical INL specification to the functions we are interested in via

$$g(z) = q\,G(z\ fs). \tag{21}$$

More specifically, the INL error in terms of the INL specification as

$$\varepsilon_{INL}\left(x_{IF}(T_s n)\right) = q\,G\left(\left(x_{IF}(T_s n) + \frac{1}{2}\right) fs\right). \tag{22}$$

We note the following important points.

- The effects of INL depend not only on the component INL specification in terms of LSB, but also on the quantization step size, i.e., the number of bits in the ADC.
- When comparing different ADC components, their INL specifications need to be 'normalized' with respect to the quantization step size *q*. That is, the proper comparison is $\varepsilon_{INL}(\ )$, and not $G(\ )$.

2.2.5 Effects of Nonlinearities on Signals

The question we answer next is "Given some INL specification $G(\ )$, and some input $x_{IF}(\ )$, what does it really do to error $\varepsilon_{INL}(\ )$?" For convenience, we shall hereafter presume the ADC full-scale $fs = 1$. It also becomes convenient to expand the INL specification into a Taylor Series about its mid-range. This yields

$$G(z) = G_0 + G_1\left(z - \frac{1}{2}\right) + G_2\left(z - \frac{1}{2}\right)^2 + G_3\left(z - \frac{1}{2}\right)^3 + \ldots + G_m\left(z - \frac{1}{2}\right)^m + \ldots, \tag{23}$$

where $G_m = \frac{1}{m!}\frac{d^m}{dz^m}G(z)\Big|_{z=1/2}$ are constant coefficients. This allows the INL error to be written as

$$\varepsilon_{INL}\left(x_{IF}(T_s n)\right) = \sum_{m=0}^{\infty} qG_m\left(x_{IF}(T_s n)\right)^m. \tag{24}$$

So, INL causes the addition of powers of the input signal. This is, as one might expect, a nonlinear function, so scaling and superposition do not hold. The constant term represents a bias. The linear term ultimately affects the scaling of the data. The problematic terms are the quadratic and higher-order terms, as they embody the nonlinearities that are particularly troublesome. Fortunately they are generally pretty small, but not without significance. Recall that $x_{IF}\left(T_s n\right)$ is real-valued. We shall now presume that the input is a single-frequency sinusoid described by

$$x_{IF}\left(T_s n\right) = A\cos\left(2\pi\left(f_d + \frac{f_s}{4}\right)T_s n\right), \tag{25}$$

where f_d is the modulation frequency offset from the IF carrier, and *A* is the amplitude of IF signal. Note that $|A| \le 1/2$, but is typically much smaller. Note again that for digital down-conversion we enjoy the IF carrier at $f_s/4$. Clearly, powers of this signal yield

$$\left(x_{IF}\left(T_s n\right)\right)^m = A^m \cos^m\left(2\pi\left(f_d + \frac{f_s}{4}\right)T_s n\right). \tag{26}$$

We recall that trig identities allow expansion of powers of a cosine to be a sum of simple cosines of scaled arguments. That is

- The expansion of $A^m \cos^m\left(\theta\right)$ contains a term $\left(A^m/2^{m-1}\right)\cos\left(m\theta\right)$.
- Specifically, $\cos^m\left(\theta\right)$ contains phase (and frequency) multiples of θ up to $m\theta$.
- Higher order terms (larger values for *m*) generally contribute lesser amounts of energy, differences in G_m notwithstanding.

This suggests that we can generally equate

$$\sum_{m=0}^{M} G_m A^m \cos^m\left(\theta\right) = \sum_{m=0}^{M} C_m\left(A\right)\cos\left(m\theta\right), \tag{27}$$

where M is the maximum value for *m* for which we have interest, and $C_m\left(A\right)$ is the polynomial function of *A*, for the m^{th} harmonic. Some algebra allows us to calculate the $C_m\left(A\right)$ as

$$C_m\left(A\right) = \begin{cases} \displaystyle\sum_{n=0}^{M/2} G_{2n} A^{2n} \frac{1}{2^{2n}}\binom{2n}{n} & m = 0 \\ \displaystyle\sum_{n=p}^{(M-1)/2} G_{2n+1} A^{2n+1} \frac{2}{2^{2n+1}}\binom{2n+1}{n-p} & m = \left(2p+1\right) \ge 1, \\ \displaystyle\sum_{n=p}^{M/2} G_{2n} A^{2n} \frac{2}{2^{2n}}\binom{2n}{n-p} & m = 2p \ge 2 \end{cases} \tag{28}$$

where *m* are defined in terms of integer values of *p*. This expansion clearly illustrates the very important point that the coefficients of $\cos\left(m\theta\right)$ are themselves polynomials of amplitude A. Even for very small *m*, the polynomials would be of exceptionally large order. This of course implies that the coefficient of any particular $\cos\left(m\theta\right)$ will observe polynomial behavior as a function of *A*. That is, as amplitude *A* increases, the coefficient of any particular $\cos\left(m\theta\right)$ may

increase, decrease, or disappear entirely. That is, the coefficient of any particular $\cos(m\theta)$ is not only nonlinear with respect *A*, it may not be even monotonic with respect to *A*. The bottom line is that, for time-varying θ, the relative strength of a particular harmonic may be highly dependent on the amplitude of the input signal. We summarize this by noting that for input signal given by Eq. (25) we identify the error due to INL for this sinusoidal input as

$$\varepsilon_{INL}\left(A\cos\left(2\pi\left(f_d+\frac{f_s}{4}\right)T_s n\right)\right)=q\sum_{m=0}^{\infty}C_m(A)\cos\left(2\pi m\left(f_d+\frac{f_s}{4}\right)T_s n\right). \tag{29}$$

We observe the following.

- Any particular $C_m(A)$ contains no terms of lower order than A^m. So, other things equal, $C_m(A)$ are likely smaller for larger *m*. However, there is no guarantee that other things are equal.
- Every instance of A^m is multiplied by G_m.
- We expect that of particular concern will be large values of G_m for low order *m*. This implies a concern for large low-frequency structure to the INL characteristic.
- Since G_m are based on a function with units *LSB*, the impact on INL error clearly depends on the number of bits in the ADC.
- The largest undesired harmonic is that for which $C_m(A)$ is the greatest, over all amplitudes *A* for $0\le A\le 1/2$ and for all $m\ge 2$.
- It is not just the peak deviation of the INL that is of concern. The underlying structure of the INL characteristic will substantially affect the nature of the harmonic content in the data.
- We reiterate an earlier point in observing that when comparing different ADC components, their INL specifications need to be 'normalized' with respect to the quantization step size *q*. That is, the proper comparison is the error $\varepsilon_{INL}(\ )$, and not the direct component specification $G(\ )$.

We also remind ourselves that insofar as the largest impact on the ultimate data, we need to take into account any attenuation by the bandwidth reduction filtering subsequent to data sampling.

2.2.6 INL Analysis Based on Energy

We now investigate the total energy in the INL distortion as generated by a sinusoidal tone. We shall again presume that the input is a sinusoidal tone, namely

$$x_{IF}(T_s n)=A\cos(\omega_n n), \tag{30}$$

where for notational convenience we use the substitution $\omega_n=2\pi(f_d+f_s/4)T_s$. The INL distortion is then given as

$$\varepsilon_{INL}\left(A\cos(\omega_n n)\right)=qG\left(A\cos(\omega_n n)+\frac{1}{2}\right). \tag{31}$$

Consequently the net distorted signal is sum of the original signal with its distortion component, that is

$$x_{ADC}(n)=A\cos(\omega_n n)+qG\left(A\cos(\omega_n n)+\frac{1}{2}\right). \tag{32}$$

We note that in this formulation the INL distortion component generally adds power to the output signal. While it does in fact modify the power at the fundamental frequency by some small amount, it also adds power at other frequencies, including zero-frequency or DC. While we are most interested in power at higher harmonics of the fundamental, this power is bounded by the total power in the INL distortion component. We calculate the power in the INL distortion component as

$$P_{INL} = q^2 \,\mathrm{mean}\left\{ G^2\left(A\cos\left(\omega_n n\right) + \frac{1}{2}\right)\right\}. \tag{33}$$

Of course, the power in the desired signal is

$$P_0 = \mathrm{mean}\left\{ A^2 \cos^2\left(\omega_n n\right)\right\} = \frac{A^2}{2}. \tag{34}$$

The relative INL distortion power level for a sinusoidal signal is then their ratio, or

$$\frac{P_{INL}}{P_0} = 2\frac{q^2}{A^2}\,\mathrm{mean}\left\{ G^2\left(A\cos\left(\omega_n n\right) + \frac{1}{2}\right)\right\}. \tag{35}$$

2.2.7 Effects on Doppler

We return to the expression for INL, but this time in terms of a generic phase,

$$\varepsilon_{INL}\left(A\cos\left(\theta\right)\right) = q\sum_{m=0}^{\infty} G_m A^m \cos^m\left(\theta\right) = q\sum_{m=0}^{\infty} C_m\left(A\right)\cos\left(m\theta\right). \tag{36}$$

In a range-Doppler image formed from data using stretch processing, signal frequency corresponds to range, and a pulse-to-pulse phase change corresponds to range-rate, or Doppler. A harmonic multiplies phase. Consequently, a harmonic of order *m* yields both a frequency multiple with factor *m* as well as a phase-rate multiple with factor *m*. That is, the m^{th} harmonic of the fundamental signal is scaled and hence shifted in both frequency and Doppler. In a range-Doppler map, it will be offset in both range *and* Doppler. In a SAR image, a Doppler offset corresponds to an azimuth position offset, whereas in a GMTI map, a Doppler offset corresponds to a velocity offset. The bottom line is that an INL spur can manifest literally all (anywhere) over the map.

2.3 Digital Down-Conversion Issues

The harmonic spurs caused by INL are generated right at the analog to digital conversion process. Consequently, unlike the main target signal, harmonic spurs are not affected at all by any analog filters earlier in the signal path. These harmonic spurs may manifest at any frequency in the raw ADC samples' frequency space. Furthermore, harmonic spurs may manifest at frequencies well beyond the ADC sampling frequency, and then be aliased down to frequencies anywhere below the ADC sampling frequency.

At the ADC component output, the raw data bandwidth is equal to the sampling frequency. The data is real-valued, so the data spectrum is unique over only half the data bandwidth. As described in earlier sections of this report, for digital down-conversion, the data spectrum of interest rides on an IF carrier that is ¼ the sampling frequency, or $f_s/4$. Subsequent to the conversion process, the data is shifted in frequency to baseband and filtered, in the process becoming complex-valued, or I/Q data. This is also known as digital demodulation followed by filtering. The filter is known as the demodulation filter, defined as $h_{demfil}\left(n\right)$ above. The key point here is that the demodulation filter has a passband width that is typically somewhat less than $f_s/4$. Subsequent digital filtering might reduce the passband even further. In any case, not all harmonic spurs will make it through these filters. At the very least some will be substantially attenuated by the digital filters' stopband performance.

As a final note, in the case of additional filtering after the demodulation filter to reduce the passband even further, such a filter may attenuate the fundamental signal, and yet still pass the appropriate harmonic. This means that in a range-Doppler map, a target outside the scene of interest can still generate harmonic spur content within the scene.

3 INL AND GMTI

We examine here the impact of INL spurs on a typical GMTI mode. Basic exo-clutter GMTI performance is discussed in a report by Doerry.[7] Basic performance parameters for DMTI are discussed in a paper by Doerry, et al.[8]

3.1 Typical GMTI Processing in a Nutshell

We shall presume a notional but typical GMTI mode that uses stretch processing, whereby the Linear FM (LFM) chirp echoes are de-chirped prior to sampling. Target energy then manifests at a constant frequency representing a constant range. Range resolution is generally coarse with respect to target dimensions. A typical raw data set for typical GMTI mode might include 1024 fast-time samples for each of 256 pulses. Fewer fast-time samples might be collected at nearer ranges. The actual number of pulses integrated will depend on radar Pulse-Repetition Frequency (PRF) and desired integration time, or Coherent Processing Interval (CPI). A 2D-DFT on the data from a collection of pulses causes the target to manifest as a point response in the range-Doppler map.

A CFAR algorithm then compares each range-Doppler pixel (in the exo-clutter region) to local noise statistics, and declares a 'detection' when a magnitude threshold is exceeded. These detections might be further filtered by subsequent detection logic involving multiple CPIs. This is often called Multiple Observation Signal Processing (MOSP). A threshold for initial detection may include criteria for Signal to Noise Ratio (SNR) and Radar Cross Section (RCS). Example detection criteria are $\mathrm{SNR} \geq 20$ dB, and $\mathrm{RCS} \geq 0$ dBsm for vehicles, and perhaps $\mathrm{RCS} \geq -10$ dBsm for dismounts.

The effect of INL distortion is to introduce other frequency components that have the same signature as legitimate targets. Consequently, INL distortion produces non-existent phantom target signatures. If a phantom target signature exceeds the detection criteria, then it is declared a detection, albeit a False Alarm detection. If the phantom target signature is not declared a detection, then it still raises the noise floor in the range-Doppler map, thereby reducing the detection probability for other targets. That is, it reduces the Probability of Detection. This is especially true if the phantom target signature contains significant energy with respect to the expected noise floor. Phantom target signatures below the noise floor are generally considered inconsequential to the detection process.

3.2 Some Basic Truths

The following basic truths will direct the subsequent analysis.

- INL spur levels depend on signal levels in a nonlinear fashion.
- INL spurs should be low enough to not generate False Alarms. They should also ideally not contribute to degradation of the Probability of Detection.
- Spur levels at or below the noise level in the range-Doppler map will be inconsequential to GMTI operation.
- Spur levels sufficiently below the minimum RCS level will be inconsequential to GMTI operation. The amount below the minimum RCS level corresponds to the minimum SNR level required for detection.
- Large RCS targets need to exhibit lower relative INL spurs than do smaller RCS targets. Consequently, spur energy level relative to signal energy (e.g. with units dBc) is signal level dependent. This falls out of an RCS threshold criterion.

3.3 Some Comments on the Range-Doppler Map

The harmonic spur analysis heretofore has generally been one-dimensional. However, as indicated above, an intermediate product for GMTI processing is a two-dimensional range-Doppler map. In such a range-Doppler map, with sufficiently high radar PRF, stationary clutter manifests itself generally as a narrow band of clutter echoes generally

extending across all ranges. This clutter band, even if centered at zero Doppler with respect to the center reference range, need not be centered at zero Doppler at all ranges. That is, the Doppler band need not be vertical in a range-Doppler map. This is explored in detail in an earlier report.[9] Furthermore, while the clutter band may be narrow, it does indeed have some width. In any case, we may expect even stationary clutter to have a significant non-zero Doppler at times. This is precisely the phenomenon exploited by SAR. Recall that harmonic spurs may be shifted in range as well as Doppler. Consequently, clutter discretes can manifest anywhere in the range-Doppler map. Furthermore, different harmonic spurs may exhibit any combination of same or different range or Doppler.

4 INL CHARACTERISTICS OF EXAMPLE ADC COMPONENT

We now examine some INL characteristics taken from a commercial ADC data sheet, and analyze its nature to evaluate expected performance in GMTI applications. The ADC is an 8-bit device with INL characteristic from its data sheet reproduced in Figure 1. Note the low-order structure. This digitized INL characteristic was subjected to simulations for harmonic spur analysis. We illustrate two examples using typical GMTI parameters. The first example collects and averages 256 vectors of 1024 samples each of a sinusoidal input with amplitude $A = 0.4$, but also without and with Additive White Gaussian Noise (AWGN) with an RMS level equal to the quantization step size q, is shown in Figure 2. Peak harmonic spurs are −64 dBc. We deem this is adequate to not cause excessive false alarms, but will degrade probability of detection.

The second example collects averages 256 vectors of 1024 samples each of a sinusoidal input but with amplitude $A = 0.1$, also with AWGN dither with an RMS level equal to the quantization step size q, is also shown in Figure 2. Peak harmonic spurs are −52 dBc. If we stipulate to detect −10 dBsm targets in the presence of +45 dBsm clutter discretes, then we can expect a false alarm. Consequently this is judged to be unsatisfactory performance.

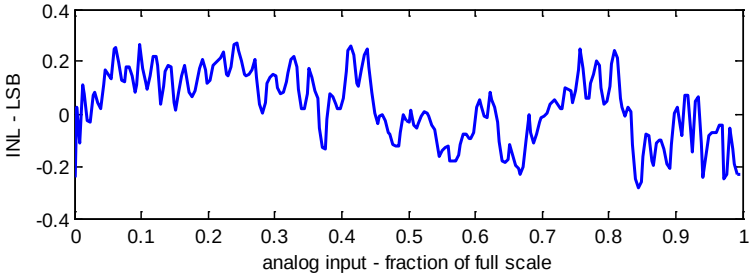

Figure 1. INL vs. output code for example ADC component.

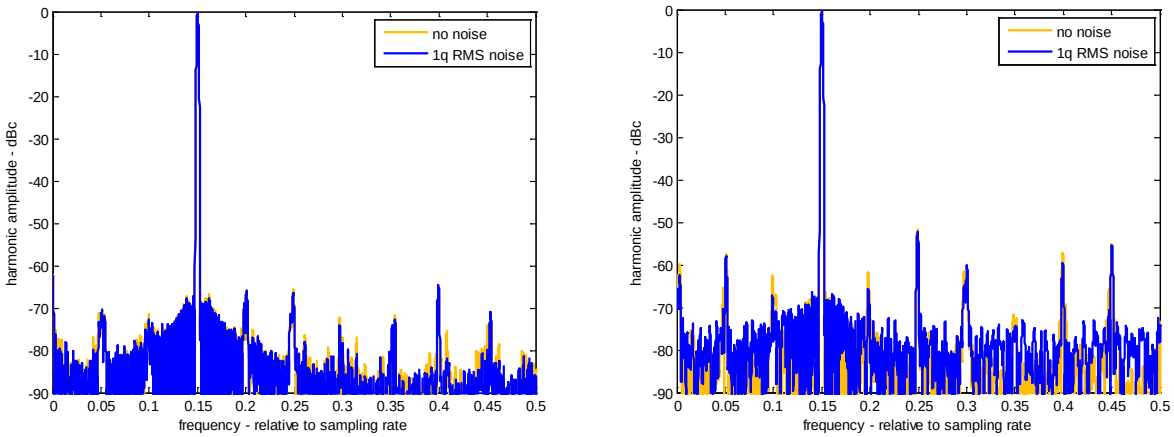

Figure 2. Spectrum of harmonic distortion produced by example ADC component INL characteristic with and without AWGN. Left plot is for signal level at *A*=0.4. Right plot is for signal level at *A*=0.1.

5 MITIGATION TECHNIQUES

Mitigation techniques for unwanted spurious energy are generally implemented with the following order of precedence.

1. Reduce or eliminate the spurious energy,
2. Move the spurious energy to unwanted signal space,
3. Smear the spurious energy to reduce its coherence and peak value, and
4. Image post-processing.

We examine these in turn, albeit in a very cursory manner. We do this by way of examples. Common parameters for all examples in this section include

8-bit ADC with INL characteristic of Figure 1.

Input signal with amplitude $A = 0.1$ relative to a maximum of 0.5.

256 pulses of 4096 samples each at ADC output.

Out-of-band Gaussian noise dither with one-sided bandwidth $0.08 f_s$, and power level with RMS value at the quantization step size.

Processing in both dimensions with a −70 dB Taylor window, with nbar = 11.

The range-Doppler map without any mitigation is illustrated in Figure 3, and exhibits a peak harmonic spur level of −52 dBc. Note that a number of spurs occur at the same range, but different Doppler locations.

5.1 Reduce or Eliminate the Spurious Energy

The harmonic spurs are a function of the linearity of the ADC conversion process. Harmonic spurs can be reduced by selecting a more linear ADC component. The important parameter is INL with respect to full scale. This can be reduced by selecting a part with the same number of bits but better INL spec, or sometimes by selecting a part with more bits even if the INL relative to the LSB increases (gets worse) somewhat. In principle, one might presume that INL can be characterized and compensated in the data. In practice, anecdotal evidence suggests that this is difficult and somewhat unreliable. Several reasons for this exist. These include

- Many high-speed ADC components multiplex the conversion to multiple internal ADC functional blocks. These internal ADC functional blocks have independent INL characteristics. It becomes somewhat problematic to assure that the right compensation goes to the right data sample.
- INL is somewhat temperature sensitive. Calibration is somewhat ‘tricky’ and would have to be done in-flight as temperature changes.
- A correction would require extending the internal busses inside the subsequent digital processors.

5.2 Move the Spurious Energy

Since INL generated harmonic spurs can exist anywhere in the overall range-Doppler map, moving some spurs outside the region of interest risks moving other harmonic spurs into the region of interest. Consequently, this is a nonviable mitigation strategy. However, if we can observe the spurs moving when the signal remains stationary, then we can identify the spurs, and perhaps neutralize them. We discuss using this to advantage in somewhat more detail later.

5.3 Smear the Spurious Energy

The most practical means of smearing the spurious energy is via phase modulation. Phase modulation is applied to the signal before the ADC conversion, and then removed from the data after conversion. Note that phase modulated harmonics in the data will be multiplied by the harmonic number, thereby multiplying the amount of phase modulation as

well. Consequently, we can expect the amount of smearing to be harmonic dependent. The kinds of phase modulation considered here are the same as were considered for I/Q balance in an earlier report.[10]

5.3.1 Range Smearing

A quadratic phase modulation in the fast-time, or range dimension will smear the harmonic spurs in range. A quadratic phase modulation is accomplished by a residual chirp. Figure 4 illustrates the effects of a residual chirp with Time-Bandwidth product of 20. The peak harmonic spur is at −68 dBc. This represents a 16 dB reduction.

5.3.2 Doppler Smearing

Doppler smearing may be accomplished by several convenient means. A Doppler chirp with Time-Bandwidth product of 20 was applied for the example of Figure 5. The peak harmonic spur is at −68 dBc. Random phase modulation on a pulse to pulse basis was applied for the example of Figure 6. The peak harmonic spur is at −67 dBc.

Random $0/\pi$ phase modulation on a pulse to pulse basis was applied for the example of Figure 7. The peak harmonic spur is at −52 dBc. Note that only odd-order harmonics are smeared. Even-order harmonics are unaffected by random $0/\pi$ phase modulation. Consequently, random $0/\pi$ phase modulation is better than nothing, but not by much.

5.3.3 Dither

Another technique to 'spread' the imbalance energy is to employ a dither signal.[11] This involves adding noise with an RMS level that is substantially greater than the nominal quantization step size. Figure 8 illustrates the effects of using an out-of-band noise dither with RMS level at 16 times the quantization level. The peak harmonic spur is at −68 dBc. A down side to this technique is that the dynamic range of the ADC itself is reduced somewhat by this additive elevated noise dither.

5.4 Range-Doppler Image Post-Processing

In GMTI modes, harmonic spurs are particularly problematic when they are large enough to be detected as false alarms. Consequently, if a particular detection can be identified as a harmonic spur, then it can be discounted as an errant detection, and not reported or processed further. One way this can be accomplished is by identifying particularly strong target responses in the range-Doppler map, and then calculating where harmonic spurs 'ought' to occur, for some number of harmonics. The detection algorithm might then be desensitized at these locations, at least sufficiently so as to not allow a false alarm. Of course problems with this are several. Among them, desensitizing the detection algorithm will also reduce the probability of detection for real targets. Additionally, typical INL specifications will generally cause a very large number of harmonic spurs that can generally be all over the range-Doppler map. Consequently, there will be a whole lot of desensitizing going on, more so yet for urban scenes that might have a large number of clutter discretes. Furthermore yet, multiple signal sources for spurs will generate intermodulation products, further complicating calculations. The bottom line is that resolving problematic INL effects in the range-Doppler map via post-processing is expected to be difficult with low probability of achieving acceptable results.

More recently, however, a spur apodization technique has been reported that shows promise, where a signal is processed simultaneously in two or more receiver channels with different modulations applied, undergoing simultaneous conversion in two or more ADCs. Modulations are chosen such that spur locations are expected to be different in the two channels even after target signal locations are registered. Consequently spur responses can be identified and mitigated.[12]

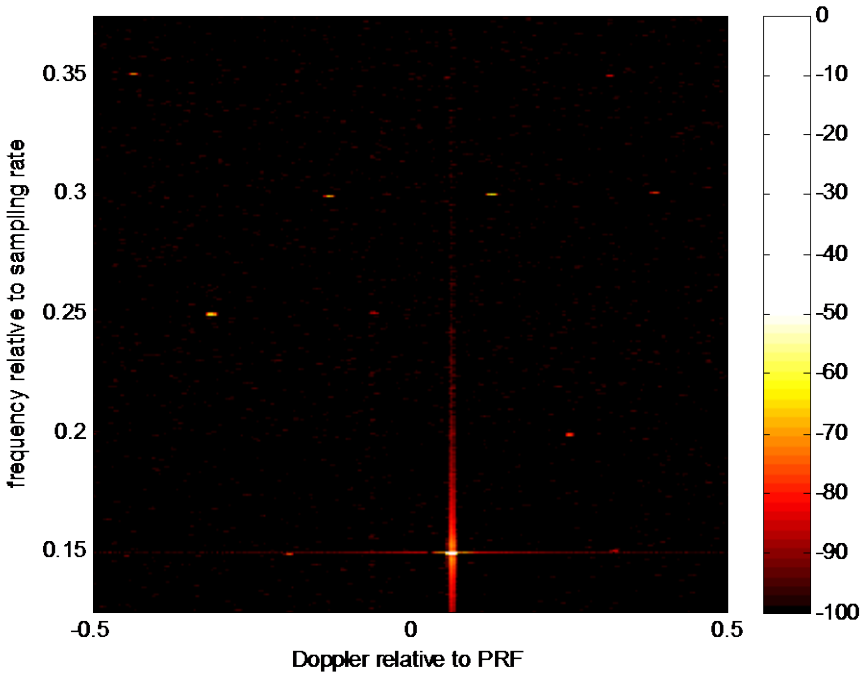

Figure 3. Range-Doppler map with INL induced harmonic spurs. The colorbar denotes dBc.

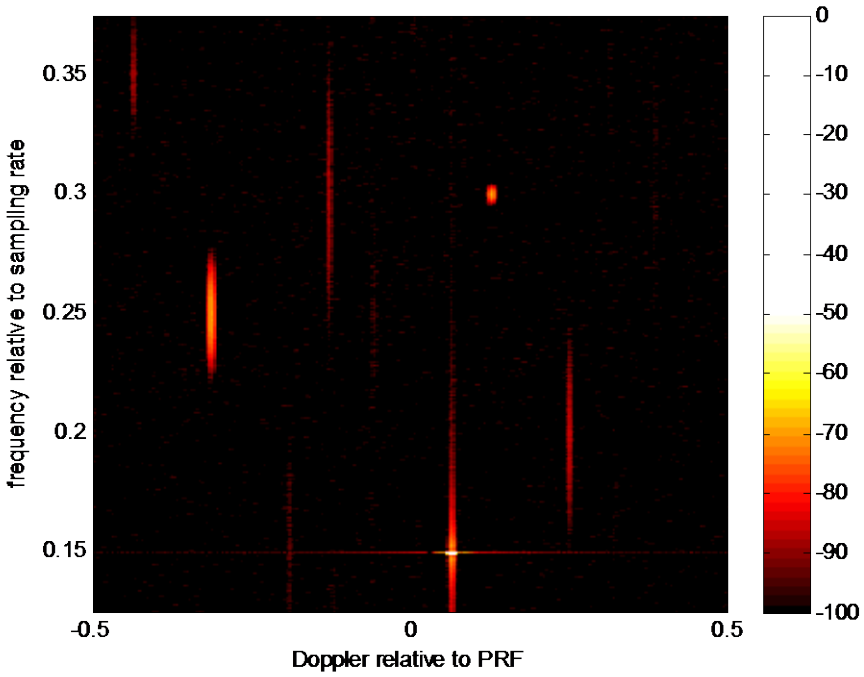

Figure 4. Range-Doppler map with INL induced harmonic spurs smeared in range by a residual chirp. The colorbar denotes dBc.

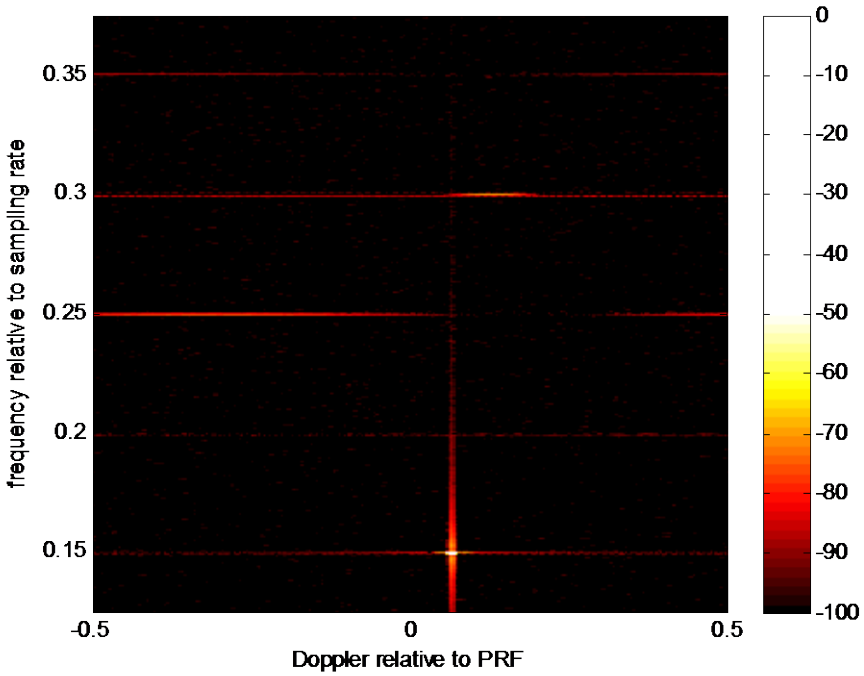

Figure 5. Range-Doppler map with INL induced harmonic spurs smeared by a Doppler chirp. The colorbar denotes dBc.

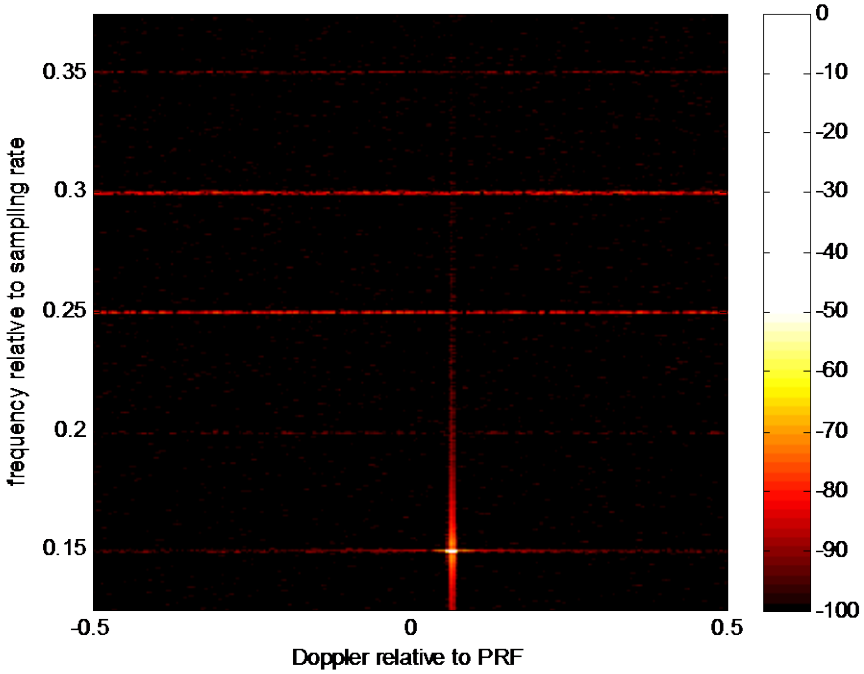

Figure 6. Range-Doppler map with INL induced harmonic spurs smeared by a pulse-to-pulse random phase modulation. The colorbar denotes dBc.

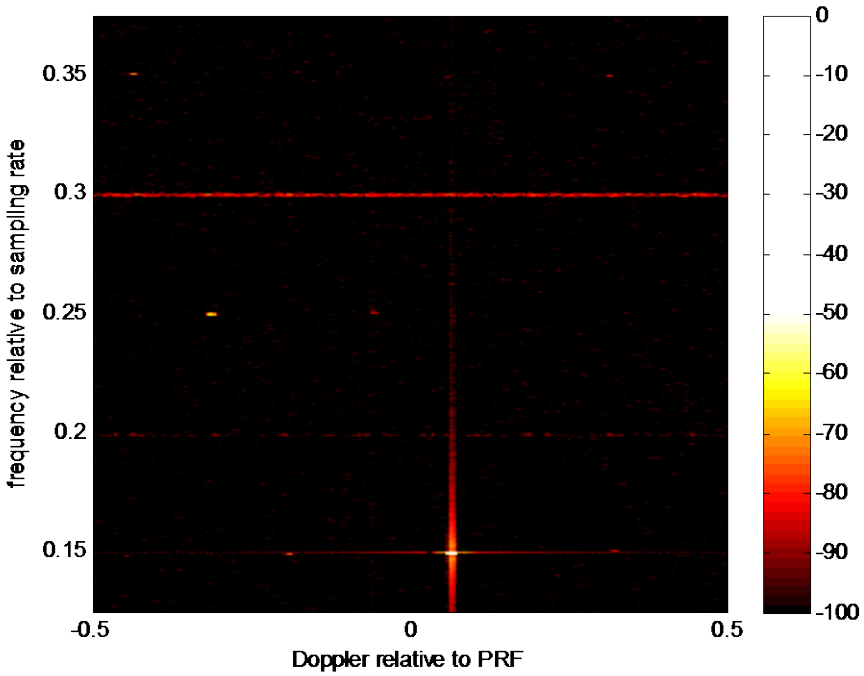

Figure 7. Range-Doppler map with INL induced harmonic spurs smeared by a pulse-to-pulse random 0/π phase modulation. The colorbar denotes dBc.

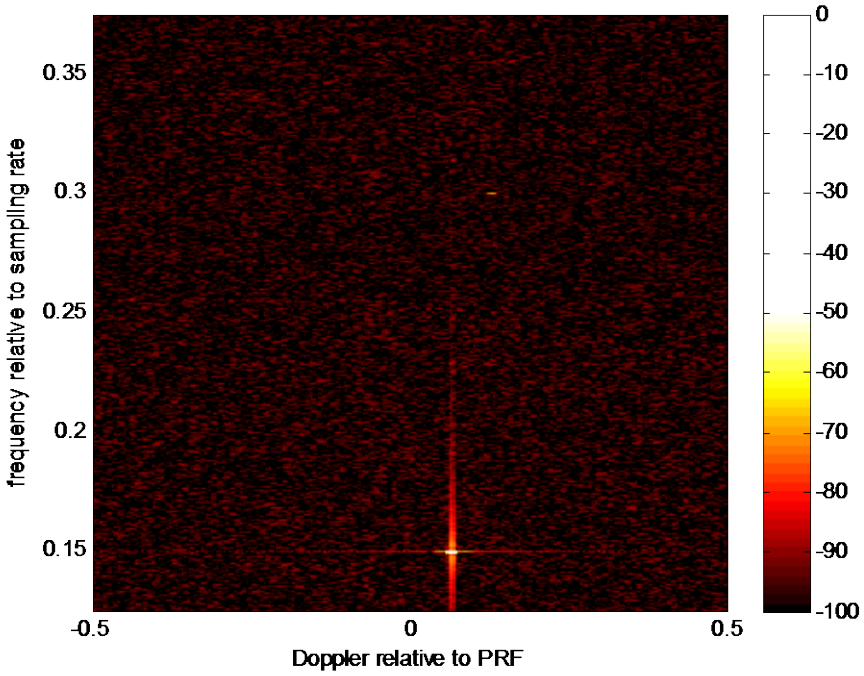

Figure 8. Range-Doppler map with INL induced harmonic spurs smeared by an elevated dither. The colorbar denotes dBc.

6 SUMMARY & CONCLUSIONS

We offer several summary comments.

- ADC INL generates harmonic spurs, which manifest as false targets in range-Doppler maps. If strong enough, they may generate false alarms in GMTI radar modes.
- Different ADCs have different INL characteristics. Lower INL characteristics are better. However, the specific harmonic content is also important.
- Mitigation techniques exist that require various radar parameter manipulations. These can substantially reduce harmonic spurs' peak levels by smearing them in range, Doppler, or both. Many of these techniques can also be used to combat effects of other system channel nonlinearities as well, such as I/Q imbalance.

ACKNOWLEDGEMENTS

Sandia National Laboratories is a multi-program laboratory managed and operated by Sandia Corporation, a wholly owned subsidiary of Lockheed Martin Corporation, for the U.S. Department of Energy's National Nuclear Security Administration under contract DE-AC04-94AL85000.

REFERENCES

[1] Ann Marie Raynal, Douglas L. Bickel, Dale F. Dubbert, Tobias J. Verge, Bryan L. Burns, Ralf Dunkel, Armin W. Doerry, "Radar cross section statistics of cultural clutter at Ku-band", SPIE 2012 Defense, Security & Sensing Symposium, Radar Sensor Technology XVI, Vol. 8361, Baltimore, MD, 23-27 April 2012.

[2] Walt Kester, "ADC Input Noise: The Good, The Bad, and The Ugly. Is No Noise Good Noise?", Analog Dialogue 40-02, February 2006.

[3] William J. Caputi, Jr., "Stretch: A Time-Transformation Technique", *IEEE Transactions on Aerospace and Electronic Systems*, Vol. AES-7, No. 2, pp 269-278, March 1971.

[4] Armin W. Doerry, Dale F. Dubbert, Bert L. Tise, "Effects of Analog-to-Digital Converter Nonlinearities on Radar Range-Doppler Maps," Sandia Report SAND2014-15909, Unlimited Release, July 2014.

[5] "INL/DNL Measurements for High-Speed Analog-to-Digital Converters (ADCs)", Application Note 283, Maxim Integrated Products, Inc., Sept. 1, 2000.

[6] Brad Brannon, Rob Reeder, "Understanding High Speed ADC Testing and Evaluation", Analog Devices Application Note AN-835.

[7] Armin W. Doerry, "Performance Limits for Exo-Clutter Ground Moving Target Indicator (GMTI) Radar", Sandia Report SAND2010-5844, Unlimited Release, September 2010.

[8] A. W. Doerry, D. L. Bickel, A. M. Raynal, "Some comments on performance requirements for DMTI radar," SPIE 2014 Defense & Security Symposium, Radar Sensor Technology XVIII, Vol. 9077, Baltimore MD, 5–9 May 2014.

[9] Armin W. Doerry, "Clutter in the GMTI Range-Velocity Map", Sandia Report SAND2009-1797, Unlimited Release, April 2009.

[10] Armin W. Doerry, "Mitigating I/Q Imbalance in Range-Doppler Images," Sandia Report SAND2014-2252, Unlimited Release, March 2014.

[11] Brad Brannon, "Overcoming Converter Nonlinearities with Dither", Analog Devices Application Note AN-410, E2096–12–12/95.

[12] Armin W. Doerry, Douglas L. Bickel, "Apodization of Spurs in Radar Receivers Using Multi-Channel Processing," Sandia Report SAND2014-1678, Unlimited Release, March 2014.